Cell Metabolism
Article

Dephosphorylation of Translation Initiation Factor 2α Enhances Glucose Tolerance and Attenuates Hepatosteatosis in Mice

Seiichi Oyadomari,[1,5] Heather P. Harding,[1,2] Yuhong Zhang,[1] Miho Oyadomari,[1,5] and David Ron[1,3,4,*]
[1]Kimmel Center for Biology and Medicine at the Skirball Institute for Biomolecular Medicine
[2]Department of Pharmacology
[3]Department of Cell Biology
[4]Department of Medicine
New York University School of Medicine, New York, NY 10016, USA
[5]Present address: Institute for Genome Research, University of Tokushima, 3-18-15 Kuramoto, Tokushima 770-8006
*Correspondence: ron@saturn.med.nyu.edu
DOI 10.1016/j.cmet.2008.04.011

SUMMARY

The molecular mechanisms linking the stress of unfolded proteins in the endoplasmic reticulum (ER stress) to glucose intolerance in obese animals are poorly understood. In this study, enforced expression of a translation initiation factor 2α (eIF2α)-specific phosphatase, GADD34, was used to selectively compromise signaling in the eIF2(αP)-dependent arm of the ER unfolded protein response in liver of transgenic mice. The transgene resulted in lower liver glycogen levels and susceptibility to fasting hypoglycemia in lean mice and glucose tolerance and diminished hepatosteatosis in animals fed a high-fat diet. Attenuated eIF2(αP) correlated with lower expression of the adipogenic nuclear receptor PPARγ and its upstream regulators, the transcription factors C/EBPα and C/EBPβ, in transgenic mouse liver, whereas eIF2α phosphorylation promoted C/EBP translation in cultured cells and primary hepatocytes. These observations suggest that eIF2(αP)-mediated translation of key hepatic transcriptional regulators of intermediary metabolism contributes to the detrimental consequences of nutrient excess.

INTRODUCTION

Eukaryotic cells respond to fluctuations in the load of unfolded proteins in the endoplasmic reticulum (ER) by an unfolded protein response (UPR). The oldest arm of the UPR, which is conserved in all eukaryotes, is mediated by IRE1, an ER stress-regulated kinase/endoribonuclease that signals through a transcription factor, XBP-1 (Hac1p in yeast), to activate UPR target genes. In animals, XBP-1 is joined by ATF6, a transcription factor that senses ER stress directly, to activate genes that enhance cells' ability to cope with the load of unfolded proteins facing their ER (reviewed in Schroder and Kaufman, 2005; Bernales et al., 2006). These transcriptional events are complemented by a third arm of the UPR mediated by PERK, an ER-localized stress-activated kinase whose only known substrate is the α subunit of translation initiation factor 2 (eIF2α). Phosphorylation of eIF2α on serine 51 inhibits the guanine nucleotide exchange factor for eIF2 and reduces rates of translation initiation. The consequent repression of protein synthesis diminishes the load of unfolded proteins entering the ER and conserves ATP and amino acids in ER-stressed cells. eIF2(αP) also activates gene expression, which is accounted for, in part, by the translational upregulation of the transcription factor ATF4 (reviewed in Ron and Harding, 2007).

Earlier studies emphasized the UPR's role in maintaining homeostasis of the protein-folding environment in the ER lumen, and its physiological significance was sought in the context of cellular adaptation to the stress posed by unfolded and misfolded ER proteins. The phenotype of mutations in components of the UPR is certainly consistent with this notion—knockout of *IRE1*, *XBP-1*, *ATF6*, and *PERK* all reduce the ability of cells to cope with ER stress (Delepine et al., 2000; Harding et al., 2001; Shen et al., 2001; Zhang et al., 2002; Lee et al., 2005; Wu et al., 2007; Yamamoto et al., 2007). However, accrued evidence now suggests that ER stress and the response to it modulate mammalian physiology in ways that cannot be explained simply by the aforementioned cell-autonomous processes.

In addition to imparting hypersensitivity to ER stress, a homozygous $Eif2a^{S51A}$ mutation (which abolishes regulatory phosphorylation of eIF2α) blocks hepatic glucose production in neonatal mice (Scheuner et al., 2001). By contrast, heterozygosity for the same $Eif2a^{S51A}$ mutation disposes adult mice to obesity, insulin resistance, and glucose intolerance (Scheuner et al., 2005). Obesity promotes ER stress, presumably by increasing the load of unfolded proteins in the ER, which is detected as enhanced UPR signaling in liver and fat (Ozcan et al., 2004; Nakatani et al., 2005). Importantly, compromised signaling in the UPR by a partial loss-of-function mutation in *XBP-1* (which further increases the level of ER stress) or a mutation in the ER chaperone ORP150 increases insulin resistance in obese mice (Ozcan et al., 2004; Nakatani et al., 2005), whereas chemical chaperones or ORP150 overexpression that reduces the level of ER stress substantially reverse the insulin resistance and glucose intolerance of obese mice (Ozawa et al., 2005; Ozcan et al., 2006). These studies imply that ER stress, or aspects of the response to it,

modulate intermediary metabolism in a manner that cannot be simply attributed to variation in survival of secretory cells.

Several kinases phosphorylate eIF2α to activate a downstream gene expression program that we refer to as the integrated stress response (ISR) (Harding et al., 2003). In yeast, a GCN2-mediated eIF2(αP)-dependent transcriptional program responds to diverse metabolic perturbations (Hinnebusch and Natarajan, 2002), and the homologous mammalian eIF2α kinase is also implicated in metabolic regulation (Hao et al., 2005; Maurin et al., 2005; Guo and Cavener, 2007). These observations suggest that links between metabolic regulation and eIF2α phosphorylation are conserved and might contribute to the physiological response to ER stress in mammals. Here we have focused on eIF2(αP) signaling in the liver, a key organ for intermediary metabolism, and present evidence that the hepatic ISR contributes to the metabolic syndrome of obesity and insulin resistance by translational upregulation of transcription factors involved in carbohydrate and lipid metabolism.

RESULTS

The major determinant of ISR activity in liver is the ER stress-activated kinase PERK, whose transient activation is difficult to detect (Harding et al., 2001). To determine whether the ISR is modulated by normal fluctuations in nutrient intake, we first monitored two perdurable markers, BiP and XBP-1 mRNA, as surrogates for the UPR (and PERK activity). Feeding coincided with a clear peak of these marker mRNAs (see Figure S1A available online), suggesting that physiological ER stress is induced by feeding, as predicted by previous studies (Dhahbi et al., 1997). To gauge the transient phosphorylation of eIF2α, we fasted animals for 18 hr and refed them with normal (low-fat) and high-fat chow. Levels of eIF2(αP) were barely detectable in liver after a 18 hr fast but increased 4 hr after feeding with ordinary chow and were even higher in animals provided high-fat chow (Figure S1B). These observations confirmed the previously noted (Ozcan et al., 2004) correlation between physiological nutritional fluctuations and the eIF2(αP)-dependent ISR in liver.

Selective Attenuation of the ISR in Liver of Transgenic Mice

To study the potential significance of physiological levels of eIF2(αP) in mouse liver, we sought to selectively interfere with this phosphorylation event. *Gadd34* (*PPP1R15a*) encodes a substrate-specific regulatory subunit of a phosphatase that selectively dephosphorylates eIF2α phosphoserine 51 (Novoa et al., 2001). *Gadd34* activity is tightly regulated at the transcriptional level, and the gene is normally turned on by the ISR as part of a negative feedback loop that terminates signaling (Novoa et al., 2003); however, enforced expression of an active C-terminal fragment of GADD34 is sufficient to dephosphorylate eIF2(αP) and inhibit the ISR (Novoa et al., 2001). We exploited this feature by expressing a GADD34 C-terminal fragment from a liver-specific albumin (*Alb*) promoter in transgenic mice. The GADD34 C-terminal active fragment (GC) was detected by immunoblot in liver lysates of transgenic *Alb::GC* mice (Figure 1A). Expression of a single copy of the transgene attenuated feeding-induced eIF2α phosphorylation, and two copies of the transgene blocked phosphorylation even during severe ER stress in mice injected with tunicamycin (Figure 1A). We conclude that the *Alb::GC* transgene interferes with eIF2α phosphorylation in the liver.

To estimate the consequences of the *Alb::GC* transgene on the eIF2(αP)-mediated ISR and to generate a hypothesis for possible mechanisms, we established a reference database for the activity of this pathway in the liver. PERK's kinase activity can be uncoupled from ER stress by fusion of the cytosolic PERK kinase domain to an artificial dimerization domain (Fv2E) that subordinates eIF2α phosphorylation to a soluble, otherwise inert ligand, AP20187 (Lu et al., 2004b) (Figure S2A). In the absence of ligand, the Fv2E-PERK chimera, expressed in the liver of transgenic mice (*Ttr::Fv2E-Perk*), is inert. However, following intraperitoneal (i.p.) injection of AP20187, the chimeric protein is activated (reflected by a shift in its mobility on SDS-PAGE) and phosphorylates its substrate (Figure 1B). The *Chop* marker gene was used to confirm the ligand and gene dose-dependent activation of the ISR in the liver of *Ttr::Fv2E-Perk* mice (Figures 1C and 1D; Figure S2B), and a profile of genes thereby induced was assembled using oligonucleotide hybridization microarrays of liver mRNA. About half of the genes previously identified as ISR targets in fibroblasts (Harding et al., 2003; Lu et al., 2004b) were also induced in the liver of the transgenic mice following injection of AP20187 ligand (Figure 1E; Table S1).

Next, we sought to determine whether the *Alb::GC* transgene, which blocked eIF2α phosphorylation, interfered with expression of this hypothesized set of ISR genes in liver. As feeding of a high-fat diet (HFD) promotes eIF2(αP) in the liver, we compared the profile of genes expressed in the liver of wild-type and *Alb::GC* mice fed high-fat or low-fat chow. As expected, the genes constituting the hepatic ISR were expressed at higher levels in the liver of HFD-fed wild-type mice. These diet-induced differences in expression were attenuated by the *Alb::GC* transgene (Figure 1E, bottom; same data in Table S2), suggesting that the latter blocks signaling in a diet-induced ISR and that such mice might constitute a useful tool for studying the role of this pathway in metabolism.

Metabolic Profile of the ISR-Defective *Alb::GC* Mice

Apart from slight gene-dosage-dependent reduced body mass (Figure 2A), adult *Alb::GC* mice were superficially indistinguishable from wild-type littermates when fed a normal diet. However, they were markedly impaired in defending blood glucose during a fast (Figure 2B). This functional defect correlated with diminished hepatic glycogen reserves (Figures 2C and 2D) and attenuated glucose production in response to pyruvate loading (a measure of gluconeogenesis) in fasted *Alb::GC* mice compared with wild-type (Figure 2E).

A tendency toward fasting hypoglycemia may also explain the high rates of perinatal attrition of *Alb::GC* transgenic mice (21 of 58 pups were found dead at postnatal day 1 in *Alb::GC* transgenic litters compared with 1 of 41 pups in the wild-type FVB/n control; $p < 0.05$ by χ^2 test), a defect they share with homozygous *Eif2a*^{S51A} mice (Scheuner et al., 2001). Consistent with these observations, *Alb::GC* mice also had enhanced glucose tolerance in experimental surrogates of the fed state, as reflected in lower serum glucose levels following i.p. injection of glucose (i.p. GTT, Figure 2F) and enhanced sensitivity to the hypoglycemic effects of injected insulin (i.p. ITT, Figure 2G).

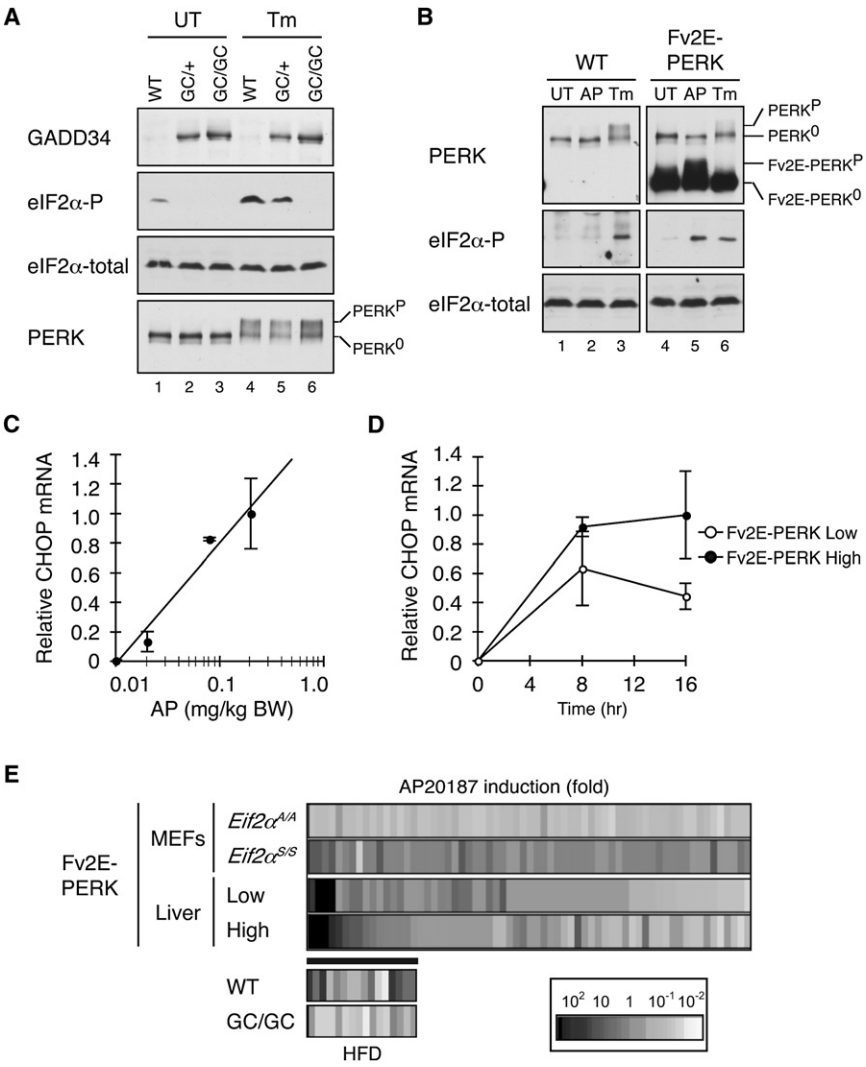

Figure 1. Enforced Dephosphorylation of eIF2α Blocks the Integrated Stress Response in the Liver of Transgenic Mice

(A) Immunoblot of immunopurified GADD34 C-terminal fragment, phosphorylated eIF2α, total eIF2α, and immunopurified PERK from liver lysates of untreated (UT) and tunicamycin-injected (Tm) nontransgenic (WT), heterozygous (GC/+), and homozygous *Alb::GC* (GC/GC) transgenic mice. The migration of inactive ($PERK^0$) and active ($PERK^P$) PERK is indicated.

(B) Immunoblot of immunopurified PERK, phosphorylated eIF2α, and total eIF2α from liver lysates of untreated (UT), AP20187-injected (AP), and tunicamycin-injected (Tm) nontransgenic (WT) and low-expressing *Ttr::Fv2E-PERK* transgenic (Fv2E-PERK) mice. The inactive and active endogenous and transgenic Fv2E-PERK proteins are labeled.

(C) Relative levels of CHOP mRNA in liver of low-expressing *Ttr::Fv2E-PERK* transgenic mice 8 hr after injection of AP20187. Shown are mean ± SEM of a representative experiment (n = 3). Linear regression analysis shows correlation factor r^2 = 0.969.

(D) Relative levels of CHOP mRNA in liver after injection of 0.2 mg/kg AP20187. Shown are mean ± SEM (n = 4) of a representative experiment performed in low- (p = 0.047 by one-way ANOVA) and high-level-expressing lines of *Ttr::Fv2E-PERK* transgenic mice (p = 0.006 by one-way ANOVA).

(E) Expression profiling of integrated stress response (ISR) target genes revealed by AP20187 treatment of *Fv2E-PERK* transgenic fibroblasts (MEFs) with wild-type ($Eif2a^{S/S}$) and mutant ($Eif2a^{A/A}$) genotypes (from Lu et al., 2004b). The induction profile of the same genes in liver of AP20187-injected *Ttr::Fv2E-PERK* transgenic mice expressing low (n = 2) and high (n = 4) levels of the transgene is shown below (data in Table S1). The inset at the bottom left depicts the expression level of a subset of these validated hepatic ISR target genes (those that are induced more than 2-fold by AP20187 expression in both *Ttr::Fv2E-PERK* transgenic lines) in high-fat diet (HFD)-fed nontransgenic (WT, n = 2) and *Alb::GC* transgenic (GC/GC, n = 2) animals (data in Table S2).

To analyze the ISR's role in the context of nutrient excess, we combined dietary manipulation with aurothioglucose injection, thus overcoming the known resistance of FVB/n mice (the background for the wild-type and transgenic mice studied here) to diet-induced obesity (Hu et al., 2004). Between 6 and 21 weeks of age, the body weight of wild-type mice increased 2.43 ± 0.16-fold, and that of the *Alb::GC* transgenic mice increased by 1.96 ± 0.08-fold (mean ± SEM, n = 12, $p < 0.05$) (Figure 3A). The resulting glucose intolerance and insulin resistance were also less in the *Alb::GC* mice compared to the wild-type mice (Figures 3B–3D). Hepatic steatosis, a predictable feature of obese wild-type male animals, was also significantly lower in ISR-defective mice fed a HFD, as reflected in a lower histochemical steatosis index of 0.8 ± 0.2 (mean ± SEM) in *Alb::GC* versus 6.4 ± 0.2 in wild-type (n = 5, $p < 0.005$; see also Figure 3E) (Kleiner et al., 2005) and lower liver tissue triglyceride content: 10.72 ± 1.69 mg/gm in *Alb::GC* versus 21.34 ± 4.11 mg/gm in wild-type (mean ± SEM, n = 5, $p < 0.05$) (Figure 3F).

The ISR Regulates Genes Involved in Intermediary Metabolism

Two transcription factors are known to be activated by eIF2(αP): ATF4, whose translation is paradoxically stimulated (Harding et al., 2000; Lu et al., 2004a; Vattem and Wek, 2004), and NF-κB, which undergoes derepression in the ISR (Jiang et al., 2003; Deng et al., 2004). However, defective signaling to their targets seemed unlikely to explain the altered hepatic gene expression program or the metabolic phenotype of the *Alb::GC* mice (Harding et al., 2003) (Table S3). Therefore, in our search for potential mediators of the metabolic effects of the ISR, we focused on other transcription factor-encoding genes that were differentially expressed in wild-type and *Alb::GC* mice. At the top of this list was peroxisome proliferator-activated receptor γ (PPARγ; *Pparg*) (Table 1).

Originally identified as an activator of adipocyte differentiation (reviewed in Rosen et al., 2000; Farmer, 2006), the nuclear receptor PPARγ has also been implicated in hepatic steatosis (Gavrilova et al., 2003; Schadinger et al., 2005). RT-PCR analysis

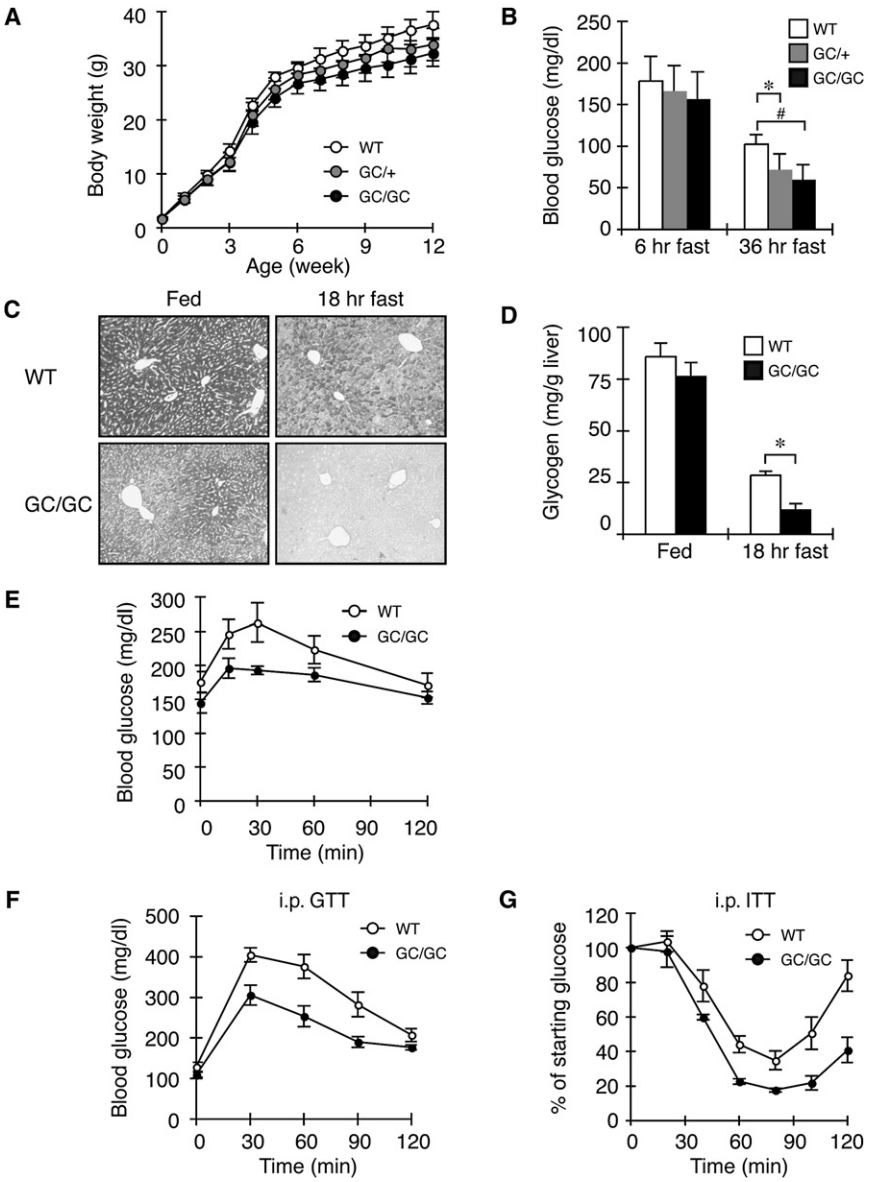

Figure 2. Fasting Hypoglycemia, Enhanced Insulin Sensitivity, and Reduced Glycogen Stores in the Liver of ISR-Defective *Alb::GC* Transgenic Mice

(A) Body weight of nontransgenic (WT), heterozygous (GC/+), and homozygous *Alb::GC* (GC/GC) transgenic male mice as function of age (mean ± SEM, n = 20).

(B) Blood glucose after fasting of adult male mice of the indicated genotypes (mean ± SEM, n = 4, *p < 0.05, #p < 0.01).

(C) Periodic acid-Schiff stain (glycogen) of representative liver sections of fed and fasted mice of the indicated genotypes.

(D) Liver glycogen content of fed and 18 hr-fasted mice of the indicated genotypes (mean ± SEM, WT n = 3, *Alb::GC* n = 5, *p < 0.05).

(E) Blood glucose levels as a function of time after pyruvate loading in mice of the indicated genotypes (mean ± SEM, n = 5, p < 0.001 by two-way ANOVA).

(F) Blood glucose as a function of time after intraperitoneal (i.p.) injection of glucose in mice of the indicated genotypes (mean ± SEM, n = 3, p < 0.001 versus WT by two-way ANOVA).

(G) Blood glucose as a function of time (expressed as a percent of level at t = 0) after i.p. injection of insulin in mice of the indicated genotypes (mean ± SEM, n = 4, p = 0.005 versus WT by two-way ANOVA).

revealed that PPARγ mRNA levels were ~2.7-fold lower in the liver of HFD-fed *Alb::GC* mice compared to wild-type (Figure 4A). Profiling also suggested a corresponding lower expression of PPARγ target genes involved in fatty acid synthesis in the *Alb::GC* transgenic mice (Table 1), which was confirmed by quantitative RT-PCR analysis of fatty acid synthetase (*Fasn*), acetyl-CoA carboxylase α and β (*Acaca* and *Acacb*), and stearoyl-CoA desaturase(*Scd1*) (Figures 4B–4E). This analysis places *Pparg* downstream of the ISR in the liver and suggests that its lower expression might contribute to reduced hepatic steatosis in *Alb::GC* transgenic mice.

Translational Activation of C/EBP Proteins by the ISR

In adipocytes, CCAAT/enhancer-binding protein β (C/EBPβ) and the related C/EBPα isoform positively regulate PPARγ expression through self-reinforcing feed-forward loops (reviewed in Rosen et al., 2000; Farmer, 2006). Recent data suggest that this relationship extends to the liver, as *Cebpb* deletion reduces levels of PPARγ2 mRNA and lipid accumulation in the liver of obese mice (Millward et al., 2007; Schroeder-Gloeckler et al., 2007). Furthermore, C/EBP proteins also promote glycogen synthesis and hepatic glucose production (Wang et al., 1995; Liu et al., 1999). These features are shared by the ISR-defective *Eif2a*^{S51A} mice (Scheuner et al., 2001) and the *Alb::GC* mice here (Figure 2 and Figure 3), prompting us to further probe the relationship of the ISR to C/EBP expression.

Levels of C/EBPβ protein were more than 2-fold lower in nuclei isolated from livers of *Alb::GC* mice than in nuclei isolated from wild-type livers, and similar differences were observed in the abundance of C/EBPα (Figures 5A and 5B). Given that the ISR regulates its best known target, ATF4, translationally (Harding et al., 2000; Lu et al., 2004a; Vattem and Wek, 2004) and that isoform choice among C/EBP proteins has previously been shown to be regulated translationally by the virally induced eIF2α kinase PKR (Calkhoven et al., 2000), we decided to determine whether the effects of the ISR on C/EBP protein levels also have a translation component.

The incorporation of [^{35}S]methionine/cysteine into newly synthesized C/EBPα and C/EBPβ was measured by pulse labeling followed by immunoprecipitation. Activation of the ISR by AP20187 in Fv2E-PERK-expressing chinese hamster ovary cells

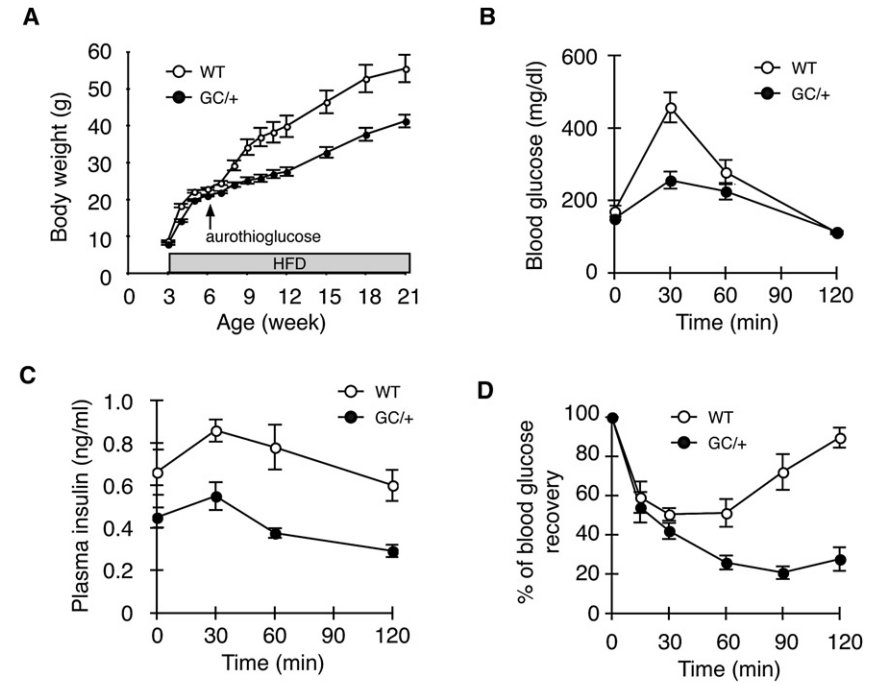

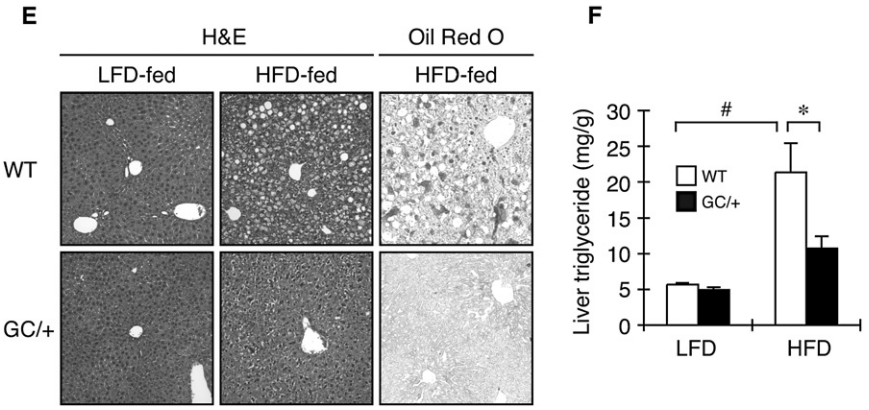

Figure 3. Sustained Insulin Sensitivity and Reduced Hepatosteatosis in ISR-Defective *Alb::GC* Transgenic Mice on a High-Fat Diet

(A) Body weight of a cohort of 12 nontransgenic (WT) and 12 *Alb::GC* transgenic mice over time (mean ± SEM, $p < 0.001$ versus WT by two-way ANOVA). High-fat diet (HFD) was instituted at weaning (3 weeks), whereas the aurothioglucose injection was introduced at 6 weeks of age.

(B) Blood glucose as a function of time after i.p. injection of glucose in obese (HFD-fed) mice of the indicated genotypes (mean ± SEM, $n = 5$, $p < 0.001$ versus WT by two-way ANOVA).

(C) Plasma insulin of the samples in (B) (mean ± SEM, $n = 5$, $p < 0.001$ versus WT by two-way ANOVA).

(D) Blood glucose as a function of time after i.p. injection of insulin in obese mice of the indicated genotypes (mean ± SEM, $n = 5$, $p < 0.001$ versus WT by two-way ANOVA).

(E) Hematoxylin and eosin (H&E) and oil red O staining of representative liver sections of mice of the indicated genotypes fed normal rodent chow (LFD) or HFD.

(F) Triglyceride content of liver from wild-type and *Alb::GC* transgenic mice fed LFD and HFD (mean ± SEM, $n = 5$, $^*p < 0.05$).

led to an ~2-fold increase in label incorporated into newly synthesized endogenous proteins (Figure 5C). This increase occurred in the face of global repression of protein synthesis, reflected here in the incorporation of label into the transcription factor CREB (Figure 5C) and eIF2α (Figure 5D). As activated Fv2E-PERK phosphorylates eIF2α without causing ER stress, these findings suggest that the ISR can enhance C/EBP translation independently of other signaling pathways.

To extend these observations to a surrogate of the liver ISR, a similar analysis was performed in HepG2 hepatoma cells in which PERK was activated by thapsigargin. Incorporation of label into newly synthesized C/EBPα and C/EBPβ increased ~2-fold within 30 min of treatment. Furthermore, the increase in translation observed over 30 min of ISR induction in the thapsigargin-treated HepG2 cells was sustained in the face of transcriptional inhibition by actinomycin D (Figure 5D), attesting to its independence of new mRNA synthesis. The effectiveness of actinomycin D in inhibiting mRNA synthesis is revealed by the block to activation of a transcriptional target of the ISR, CHOP (Figure 5D, inset).

To determine whether attenuating the ISR by *Alb::GC* expression affects translational induction of C/EBP in hepatocytes, we compared the incorporation of labeled methionine/cysteine into C/EBPβ in untreated and thapsigargin-treated primary hepatocytes explanted from wild-type and *Alb::GC* transgenic mice. Thapsigargin reproducibly enhanced the incorporation of label into immunopurified C/EBPβ in wild-type, but not *Alb::GC* transgenic, hepatocytes (Figures 5E and 5F). As expected, attenuation of total protein synthesis by thapsigargin was also less conspicuous in the *Alb::GC* transgenic sample. The rapid dedifferentiation of cultured primary hepatocytes likely leads to an underestimate of the transgene's effect in vivo. Dedifferentiation may also account for our inability to detect labeled C/EBPα in these samples.

The physiological significance of regulated expression of C/EBP isoforms by the ISR is supported by the finding that genes encoding key enzymes in hepatic glucose metabolism that are known to be regulated by C/EBPs were reduced in the *Alb::GC* transgenic mice. This relationship extended across a range of physiological states from normal feeding (Figure 5G) to animals in which diabetes mellitus had been induced by streptozotocin injection (Figure 5H).

Expression profiling revealed that many ISR target genes were induced to lower levels in the livers of transgenic mice from the line expressing more Fv2E-PERK (Figure 1E; Table S1). This finding suggested negative feedback in the ISR, for example by CHOP, a late downstream transcription factor induced by the ISR (Harding et al., 2000) that inhibits conventional C/EBP target

genes (Ron and Habener, 1992) and blocks adipocytic differentiation (Batchvarova et al., 1995), or another transcriptional target of the ISR, ATF3, which inhibits ATF4 (Jiang et al., 2004). To explore this suggestion of biphasic regulation of gene expression by the ISR, we injected *Ttr::Fv2E-PERK* transgenic animals (of the lower-expressing line) with increasing amounts of the AP20187 activator and measured mRNA levels in their livers by RT-PCR. While CHOP, ATF3, and C/EBPβ mRNA levels increased monophasically with AP20187 dose, other genes such as *Pparg*, *Pck1* (*Pepck*), and other C/EBP target genes responded biphasically (Figure 6A). These observations suggest that at lower levels of signaling, the ISR contributes positively to the regulation of the same metabolic pathways that it inhibits at unusually high, possibly pathological, levels of signaling.

DISCUSSION

By focusing on one branch of the UPR—the eIF2(αP)-mediated ISR—and by restricting the genetic manipulation to a single tissue—the liver—this study clarifies earlier work in mice with pervasive alterations in the ER stress response that were effected by germline mutations in UPR pathway genes. Both the hepatic ISR-defective *Alb::GC* mice described here and globally ISR-defective homozygous *Eif2a*^{S51A} mutant mice (Scheuner et al., 2001) share a tendency toward fasting hypoglycemia and reduced hepatic glycogen content. This argues that at least some of the metabolic consequences of a defective ISR are autonomous to the hepatocyte.

The aforementioned hepatic defect is well explained by lower levels of C/EBPα and β protein in the liver of *Alb::GC* mice, as both C/EBPα and β are known to positively regulate genes involved in glycogen synthesis and hepatic glucose production (Wang et al., 1995; Liu et al., 1999). Our findings argue that ISR-mediated activation of C/EBPα and β can proceed by a translational mechanism that is mobilized within minutes of induction of eIF2α phosphorylation and functions independently of new mRNA synthesis. Translational activation is aided by previously recognized transcriptional upregulation, which likely reinforces further C/EBP expression (Chen et al., 2004). In these respects, the C/EBPs resemble the well-validated translational target of the mammalian ISR, ATF4, and its yeast counterpart, GCN4. However, the arrangement of conserved upstream open reading frames in the C/EBPα and β genes suggests important differences between the molecular mechanism by which eIF2(αP) promotes their translation and that of ATF4/GCN4. Two conserved upstream open reading frames specify regulated translational reinitiation at the ATF4 (and GCN4) coding sequence when levels of phosphorylated eIF2α are high (Hinnebusch and Natarajan, 2002; Lu et al., 2004a; Vattem and Wek, 2004). In the case of C/EBPα and β, our observations and those of Calkhoven and colleagues (2000) are more readily explained by a model whereby eIF2(αP) disfavors initiation at the single inhibitory short open reading frame conserved in their mRNAs and favors initiation at one or more downstream AUGs. The mechanism linking eIF2(αP) to regulated initiation at two consecutive open reading frames remains to be resolved; however, the phenomenon is not restricted to C/EBPα and β, as it is observed on the ATF4 mRNA when the 5′-most of the two upstream open reading frames is deleted (see Figure 5B in Lu et al., 2004a).

Our study also implicates the ISR in regulating lipid metabolism in the liver, as *Alb::GC* mice accumulated less neutral lipid in their livers when placed on a HFD. This alteration, too, appears to be mediated by changes in gene expression, as levels of enzymes involved in fatty acid synthesis were lower in the ISR-defective transgenic mice compared with the wild-type. Lower levels of PPARγ might explain part of this defect, as a requirement for hepatic PPARγ in the development of hepatic steatosis has been noted recently (Gavrilova et al., 2003). C/EBP proteins positively regulate PPARγ expression (Millward et al., 2007; Rahman et al., 2007), which is consistent with a linear pathway from eIF2(αP) to the C/EBP proteins and from there to PPARγ (Figure 6B). Furthermore, the ISR-defective *Alb::GC* transgenic mice gain significantly less weight when placed on a HFD. While a detailed understanding of the physiological mechanisms awaits further studies, the pervasive role of eIF2(αP) in regulating genes involved in glycogenesis and lipid synthesis is consistent with the idea that impaired conversion of ingested nutrients to their storage forms limits weight gain in these ISR-defective animals.

In cultured cells, transient activation of the ISR promotes survival and adaptation whereas unremitting signaling promotes cell death (Rutkowski et al., 2006). The observations made here provide an interesting parallel in terms of intermediary metabolism in the liver: low-level signaling in the ISR (as observed under physiological circumstances) promotes expression of genes involved in glycogen synthesis, gluconeogenesis, and fatty acid synthesis, whereas higher levels of signaling repress the expression of the same genes. These findings might be explained by differential responsiveness of the ISR's effectors to signaling at different intensities, as proposed by Rutkowski et al. (2006). CHOP, ATF3, and C/EBPβ mRNA levels increase monophasically with signal strength, but expression of downstream C/EBP target genes declines at high levels of ISR activity (Figure 6A). CHOP-mediated inhibition of C/EBP proteins (Ron and Habener, 1992) and direct repression of PEPCK by ATF3 (Allen-Jennings et al., 2002) could contribute to the declining limb of the biphasic relationship between strength of ISR signal and downstream target gene expression.

Biphasic regulation of enzymes involved in fatty acid biosynthesis may also explain an apparent discrepancy between this study, in which signaling in the hepatic ISR is shown to promote steatosis in mice fed a HFD, and the observation that global *Gcn2* deletion predisposes mice fed a leucine-deficient diet to steatosis (Guo and Cavener, 2007). Perhaps leucine deficiency is associated with levels of ISR signaling that repress lipid synthesis in wild-type mice but fail to achieve this level in *Gcn2*$^{-/-}$ mice. Alternatively, the lower levels of amino acid transporters noted in ISR-defective cells (Harding et al., 2003) may further reduce hepatic uptake of leucine and sensitize amino acid-deprived *Gcn2*$^{-/-}$ mice to fatty liver by further reducing the building blocks for lipoprotein synthesis and thereby lipid export.

It has previously been reported that a partial compromise in downstream signaling in the IRE1 branch of the UPR (effected by haploid insufficiency for *Xbp1*) accentuates insulin resistance and promotes glucose intolerance in obese mice (Ozcan et al., 2004) and that protein and chemical chaperones that reduce ER stress in insulin target tissues ameliorate that phenotype (Ozawa et al., 2005; Ozcan et al., 2006). Our study suggests

Table 1. List of Genes Discordantly Regulated by High-Fat Feeding in Wild-Type and *Alb::GC* Mice

			Expression Level						
			WT		*Alb::GC*		HFD Induction (Fold)		
Name	Description	Entrez Gene	LFD	HFD	LFD	HFD	WT HFD/LFD	*Alb::GC* HFD/LFD	% of WT in GC HFD
Transcription Factors									
Pparg	peroxisome proliferator-activated receptor gamma	19016	0.97 ± 0.28	4.05 ± 0.04	0.68 ± 0.71	0.25 ± 0.11	4.18 ± 1.03	0.37 ± 0.13	6 ± 2
Crsp6	cofactor required for Sp1 transcriptional activation, subunit 6	234959	0.69 ± 0.13	2.29 ± 0.51	1.02 ± 0.33	0.65 ± 0.22	3.30 ± 0.09	0.63 ± 0.01	28 ± 3
Jarid1d	jumonji, AT rich interactive domain 1D (Rbp2-like)	20592	0.49 ± 0.14	1.38 ± 1.14	1.74 ± 3.07	0.45 ± 0.35	2.84 ± 1.01	0.26 ± 0.12	32 ± 1
Klf13	Krüppel-like factor 13	50794	0.65 ± 0.27	4.20 ± 0.19	0.87 ± 0.16	1.41 ± 0.63	6.44 ± 1.95	1.61 ± 0.33	33 ± 11
Ppara	peroxisome proliferator-activated receptor alpha	19013	0.83 ± 0.13	5.41 ± 0.29	0.61 ± 0.26	1.82 ± 1.35	6.51 ± 0.57	2.99 ± 0.59	34 ± 18
Sox-4	SRY-box containing gene 4	20677	0.86 ± 0.45	2.93 ± 0.60	0.67 ± 0.02	1.02 ± 0.53	3.41 ± 0.81	1.54 ± 0.61	35 ± 8
Nfic	nuclear factor I/C	18029	0.47 ± 0.05	3.80 ± 0.38	0.59 ± 0.03	1.67 ± 0.35	8.04 ± 0.01	2.81 ± 0.40	44 ± 4
Cphx	cytoplasmic polyadenylated homeobox	105594	0.28 ± 0.37	1.55 ± 0.62	0.13 ± 0.04	0.69 ± 0.22	5.49 ± 2.81	5.24 ± 0.12	44 ± 3
Akna	AT-hook transcription factor	100182	0.39 ± 0.24	1.69 ± 0.48	0.60 ± 0.14	0.79 ± 0.25	4.33 ± 1.79	1.31 ± 0.35	47 ± 6
Mxd3	Max dimerization protein 3	17121	0.29 ± 0.06	1.10 ± 0.09	0.54 ± 0.23	0.56 ± 0.52	3.84 ± 0.44	1.04 ± 0.32	51 ± 31
Mef2a	myocyte enhancer factor 2A	17258	0.27 ± 0.02	1.73 ± 0.19	0.51 ± 0.81	0.96 ± 0.32	6.39 ± 0.29	1.88 ± 1.33	55 ± 10
Klf3	Krüppel-like factor 3 (basic)	16599	0.74 ± 0.04	1.74 ± 0.08	0.93 ± 0.04	1.04 ± 0.17	2.37 ± 0.01	1.12 ± 0.12	60 ± 6
Nfkb2	NF-kappaB2/p100	18034	0.27 ± 0.03	3.27 ± 0.10	0.32 ± 0.00	1.98 ± 0.36	11.93 ± 0.81	6.27 ± 0.97	61 ± 8
Bach2	BTB and CNC homology 2	12014	0.52 ± 0.62	1.90 ± 0.18	0.50 ± 0.11	1.16 ± 0.39	3.66 ± 2.73	2.29 ± 0.23	61 ± 12
Zkscan1	zinc finger with KRAB and SCAN domains 1	74570	0.73 ± 0.14	1.60 ± 0.05	0.98 ± 0.04	1.11 ± 0.14	2.20 ± 0.33	1.13 ± 0.09	69 ± 6
Carbohydrate Metabolism									
Pdha2	pyruvate dehydrogenase E1 alpha 2	18598	0.16 ± 0.02	0.37 ± 0.26	0.23 ± 0.14	0.14 ± 0.06	2.26 ± 1.01	0.61 ± 0.07	39 ± 7
Pdk3	pyruvate dehydrogenase kinase, isoenzyme 3	236900	0.33 ± 0.02	0.87 ± 0.09	0.38 ± 0.05	0.37 ± 0.06	2.61 ± 0.14	0.98 ± 0.03	42 ± 3
Mdh2	malate dehydrogenase 2, NAD (mitochondrial)	17448	0.75 ± 0.18	1.91 ± 0.10	0.64 ± 0.04	1.11 ± 0.04	2.54 ± 0.42	1.72 ± 0.04	58 ± 1
Agl	amylo-1, 6-glucosidase, 4-alpha-glucanotransferase	77559	0.85 ± 0.13	1.85 ± 0.07	0.71 ± 0.04	1.09 ± 0.09	2.17 ± 0.23	1.54 ± 0.03	59 ± 2
Ppp2r5e	protein phosphatase 2, regulatory subunit B (B56), epsilon	26932	0.43 ± 0.03	2.57 ± 0.19	0.45 ± 0.35	1.52 ± 0.40	6.00 ± 0.02	3.37 ± 1.17	59 ± 10

Table 1. *Continued*

			Expression Level						
			WT		*Alb::GC*		HFD Induction (Fold)		
Name	Description	Entrez Gene	LFD	HFD	LFD	HFD	WT HFD/LFD	*Alb::GC* HFD/LFD	% of WT in GC HFD
Ppp1r1a	protein phosphatase 1, regulatory (inhibitor) subunit 1A	58200	0.60 ± 0.11	1.39 ± 0.04	0.79 ± 0.10	0.84 ± 0.20	2.33 ± 0.32	1.07 ± 0.09	61 ± 11
Gyg	glycogenin	27357	0.68 ± 0.09	1.99 ± 0.12	0.31 ± 0.61	1.26 ± 0.20	2.93 ± 0.18	4.11 ± 4.48	63 ± 6
Pcx	pyruvate carboxylase	18563	0.72 ± 0.07	1.90 ± 0.08	0.72 ± 0.11	1.19 ± 0.08	2.64 ± 0.17	1.66 ± 0.20	63 ± 2
Pklr	pyruvate kinase liver and red blood cell	18770	0.66 ± 0.09	1.67 ± 0.10	0.99 ± 0.15	1.11 ± 0.06	2.53 ± 0.25	1.12 ± 0.07	66 ± 3
Gbe1	glucan (1,4-alpha-), branching enzyme 1	74185	0.60 ± 0.01	2.07 ± 0.17	0.71 ± 0.01	1.40 ± 0.14	3.43 ± 0.22	1.96 ± 0.15	68 ± 1
Suclg2	succinate-coenzyme A ligase, GDP-forming, beta subunit	20917	0.73 ± 0.02	1.59 ± 0.03	0.84 ± 0.06	1.13 ± 0.04	2.17 ± 0.02	1.34 ± 0.05	71 ± 1
Lipid Metabolism									
Scd1	stearoyl-coenzyme A desaturase 1	20249	0.81 ± 0.19	3.43 ± 0.11	1.18 ± 0.25	0.90 ± 0.10	4.24 ± 0.77	0.76 ± 0.06	26 ± 2
Fasn	fatty acid synthase	14104	0.85 ± 0.25	2.26 ± 0.09	0.98 ± 0.08	0.88 ± 0.06	2.66 ± 0.58	0.90 ± 0.01	39 ± 1
Gpd2	glycerol phosphate dehydrogenase 2, mitochondrial	14571	0.86 ± 0.29	1.86 ± 0.05	0.89 ± 0.03	0.84 ± 0.24	2.17 ± 0.58	0.95 ± 0.21	45 ± 10
Lpl	lipoprotein lipase	16956	0.66 ± 0.15	1.96 ± 0.68	0.83 ± 0.36	0.93 ± 0.48	2.95 ± 0.27	1.13 ± 0.06	48 ± 6
Olah	oleoyl-ACP hydrolase	99035	0.12 ± 0.00	0.34 ± 0.07	0.12 ± 0.01	0.17 ± 0.05	2.82 ± 0.47	1.43 ± 0.27	50 ± 4
Acaca	acetyl-coenzyme A carboxylase alpha	107476	0.62 ± 0.43	1.82 ± 0.30	0.71 ± 0.02	1.11 ± 0.19	2.94 ± 1.12	1.58 ± 0.20	61 ± 0
Gyk	glycerol kinase	14933	0.53 ± 0.04	1.84 ± 0.06	0.69 ± 0.16	1.16 ± 0.00	3.46 ± 0.16	1.68 ± 0.35	63 ± 2
Hadh	hydroxyacyl-coenzyme A dehydrogenase	15107	0.32 ± 0.16	2.78 ± 0.02	0.25 ± 0.02	1.87 ± 0.44	8.57 ± 3.53	7.45 ± 0.94	67 ± 14
Translation, Amino Acid Import, and Metabolism									
Eif3s6	eukaryotic translation initiation factor 3, subunit 6	16341	0.42 ± 0.11	1.03 ± 0.18	0.81 ± 0.92	0.33 ± 0.11	2.43 ± 0.14	0.41 ± 0.21	32 ± 4
Aoc3	amine oxidase, copper containing 3	11754	0.21 ± 0.04	0.67 ± 1.23	0.55 ± 1.35	0.19 ± 0.05	3.17 ± 3.17	0.35 ± 0.42	29 ± 26
Pgd	phosphogluconate dehydrogenase	110208	0.91 ± 0.18	2.04 ± 0.05	1.00 ± 0.11	0.82 ± 0.02	2.24 ± 0.35	0.82 ± 0.06	40 ± 0
Rps18	ribosomal protein S18	20084	0.61 ± 0.11	2.39 ± 2.01	1.03 ± 0.09	0.96 ± 0.08	3.91 ± 1.77	0.93 ± 0.01	40 ± 22
RPL39L	ribosomal protein L39-like	68172	0.50 ± 0.20	1.32 ± 0.71	0.12 ± 0.03	0.75 ± 0.03	2.65 ± 0.26	6.33 ± 1.31	57 ± 23
Slc12a1	solute carrier family 12, member 1	20495	0.16 ± 0.10	1.80 ± 0.07	0.57 ± 0.84	1.25 ± 1.38	11.52 ± 5.41	2.22 ± 0.37	70 ± 53
Tph1	tryptophan hydroxylase 1	21990	0.44 ± 0.14	1.40 ± 0.34	1.25 ± 0.55	0.99 ± 0.43	3.22 ± 0.23	0.79 ± 0.00	71 ± 10

Shown are genes induced ≥2-fold by high-fat diet (HFD) feeding in wild-type (WT) mice and reduced by at least 25% in HFD-fed *Alb::GC* transgenic mice compared to HFD-fed WT. "HFD induction" is the ratio of the hybridization signals in HFD-fed versus low-fat diet (LFD)-fed mice. "% of WT in GC HFD" is the percentage of the signal of HFD-fed WT observed in HFD-fed *Alb::GC* (GC) mice. The mean ± standard deviation of the expression level (see Experimental Procedures) in WT and *Alb::GC* from two independent mice is shown. The uppermost cluster is a list of genes encoding transcription factors that satisfy the above criteria but are also induced ≥2-fold in AP20187-injected (0.2 μg/gm body weight) high-expressing *Ttr::Fv2E-PERK* (line #30) transgenic mice. The three clusters below list genes involved in carbohydrate, lipid, and amino acid metabolism that satisfy the above criteria.

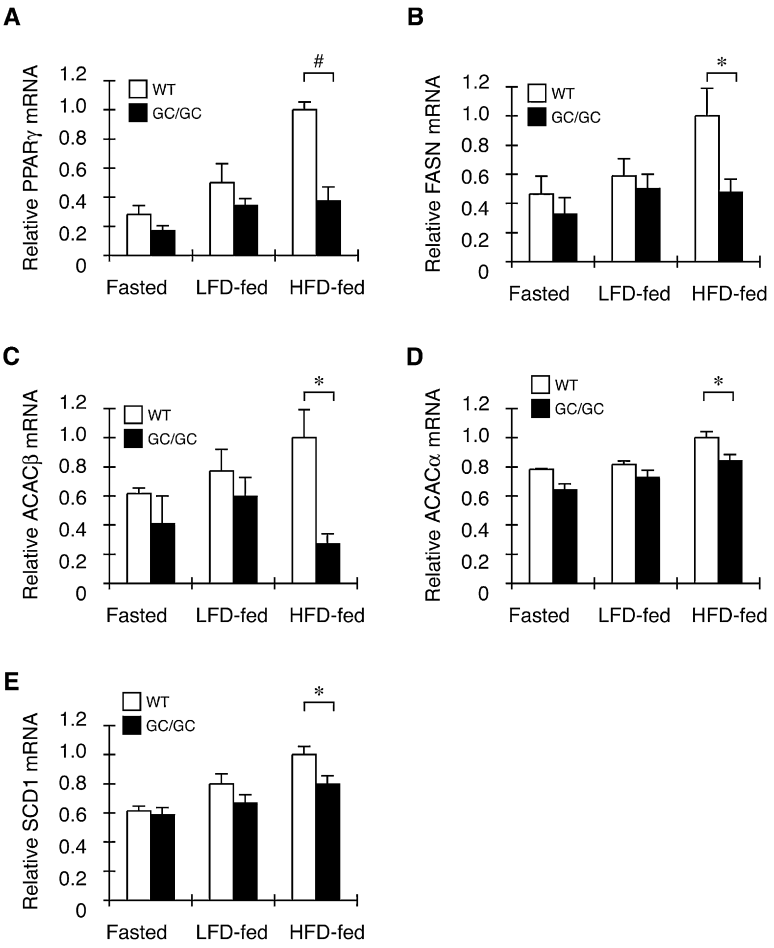

Figure 4. Reduced Expression of PPARγ and Its Target Lipogenic Enzymes in the Liver of ISR-Defective *Alb::GC* Transgenic Mice on a High-Fat Diet

Relative levels of PPARγ (A), FASN (B), ACACβ (C), ACACα (D), and SCD1 (E) mRNA in the liver of nontransgenic (WT) and *Alb::GC* transgenic mice in the fasted state or fed a low-fat diet (LFD) or high-fat diet (HFD) (mean ± SEM, n = 3–4, *p < 0.05).

a parallel process operating in hepatocytes, whereby heightened activity of the ISR and its downstream target genes contributes to the link between (physiological) ER stress and the metabolic syndrome of obesity and diabetes. In regard to intermediary metabolism, signaling by IRE1 and the ISR proceed in parallel, and neither seems to dominate the metabolic phenotype. This is exemplified by observations that insulin signaling to its proximal targets is not obviously affected by the ISR perturbation (data not shown), whereas such a defect is predicted in a system dominated by IRE1 signaling. Though loss of translational control in the ISR-defective state leads to more IRE1 signaling, which impairs insulin signaling, our study suggests that the net effect of a compromised ISR is to ameliorate the metabolic phenotype in mice exposed to nutrient excess.

It is interesting to speculate on the evolutionary origins of the link between the ISR and intermediary metabolism. Gene knockout experiments show that in most mammalian tissues, the ER stress-inducible kinase PERK dominates ISR activity (Harding et al., 2001). However, the GCN2-posessing ancestor in which PERK first evolved already had in place a gene expression program responsive to eIF2(αP) that modulated intermediary metabolism (Hinnebusch and Natarajan, 2002). We propose that this preexisting link was co-opted by PERK to coordinate intermediary metabolism with nutritionally entrained variation in load of unfolded client proteins that enter the ER of insulin-responsive tissues. This model is supported by the observation that yeasts, which lack PERK, also use ER activity as a proxy for nutrient availability but effect this by IRE1 signaling (Schroder et al., 2000; Patil et al., 2004). Presumably, under conditions of limited nutrient availability, this fine tuning of intermediary metabolism by physiological levels of ER stress signaling is adaptive; however, in the presence of excess nutrients, the ISR's contributions to lipid synthesis and hepatic glucose production are counterproductive and promote glucose intolerance and liver steatosis. Time will tell whether this example of failure of homeostasis can be exploited therapeutically, by targeting distinct facets of the ISR with inhibitors.

EXPERIMENTAL PROCEDURES

Transgenic Mice

A 2.3 kb mouse albumin enhancer/promoter fragment was used to drive expression of hamster GADD34 (aa 292–590) in the *Alb::GC* transgene. Two transgenic lines, #14 and #16, were established in the FvB/n strain. These lines exhibited similar sensitivity to fasting hypoglycemia, and the higher-expressing line, #14, was used in subsequent studies.

As we were unable to obtain lines expressing Fv2E-PERK using the *Alb* promoter, the transthyretin (*Ttr*) promoter was used instead to produce six *Ttr::Fv2E-Perk* transgenic lines in FvB/n, two of which, expressing the protein at different levels (#30 "high" and #58 "low"; Figure S2B), were selected for further study. For the experiment reported in Table S3, the low-expressing *Ttr::Fv2E-Perk* transgenic line (#58) was bred into the *Atf4* knockout strain, the derivative compound heterozygous mice (in the mixed FvB/n; Swiss Webster background) were backcrossed to the $Atf4^{+/-}$ parental stock, and *Ttr::Fv2E-PERK*-positive siblings with $Atf4^{+/+}$ and $Atf4^{-/-}$ genotypes were analyzed.

Animal Experiments

All experiments in mice were approved by the New York University School of Medicine Institutional Animal Care and Use Committee. Because of their enhanced susceptibility to the metabolic consequences of nutrient excess, male mice were used. These animals were maintained on low-fat diet (LFD) containing 12% fat or high-fat diet (HFD) containing 60% fat (Research Diets #D12492) with 12 hr light and dark cycles.

To induce hypoinsulinemic diabetes, streptozotocin (100 mg/kg, Sigma) freshly dissolved in citrate buffer (pH 4.5) was injected i.p. into 10- to 12-week-old mice on 2 consecutive days.

For diet-induced obesity, aurothioglucose (0.5 mg/g, Schering-Plough) was injected i.p. as a single dose into 6-week-old mice.

For the glucose tolerance test, mice were fasted overnight (14 hr) and injected i.p. with a glucose solution (2 g/kg). For the insulin tolerance test, mice were fasted for 4 hr and injected i.p. with human insulin (0.75 mU/kg, Eli Lilly). For pyruvate loading, mice were fasted for 16 hr and injected i.p. with 1.5 g/kg sodium pyruvate. Blood glucose and plasma insulin concentrations were measured from tail blood using a OneTouch Ultra glucometer (Johnson & Johnson) and a rat/mouse insulin ELISA kit (Linco Research), respectively.

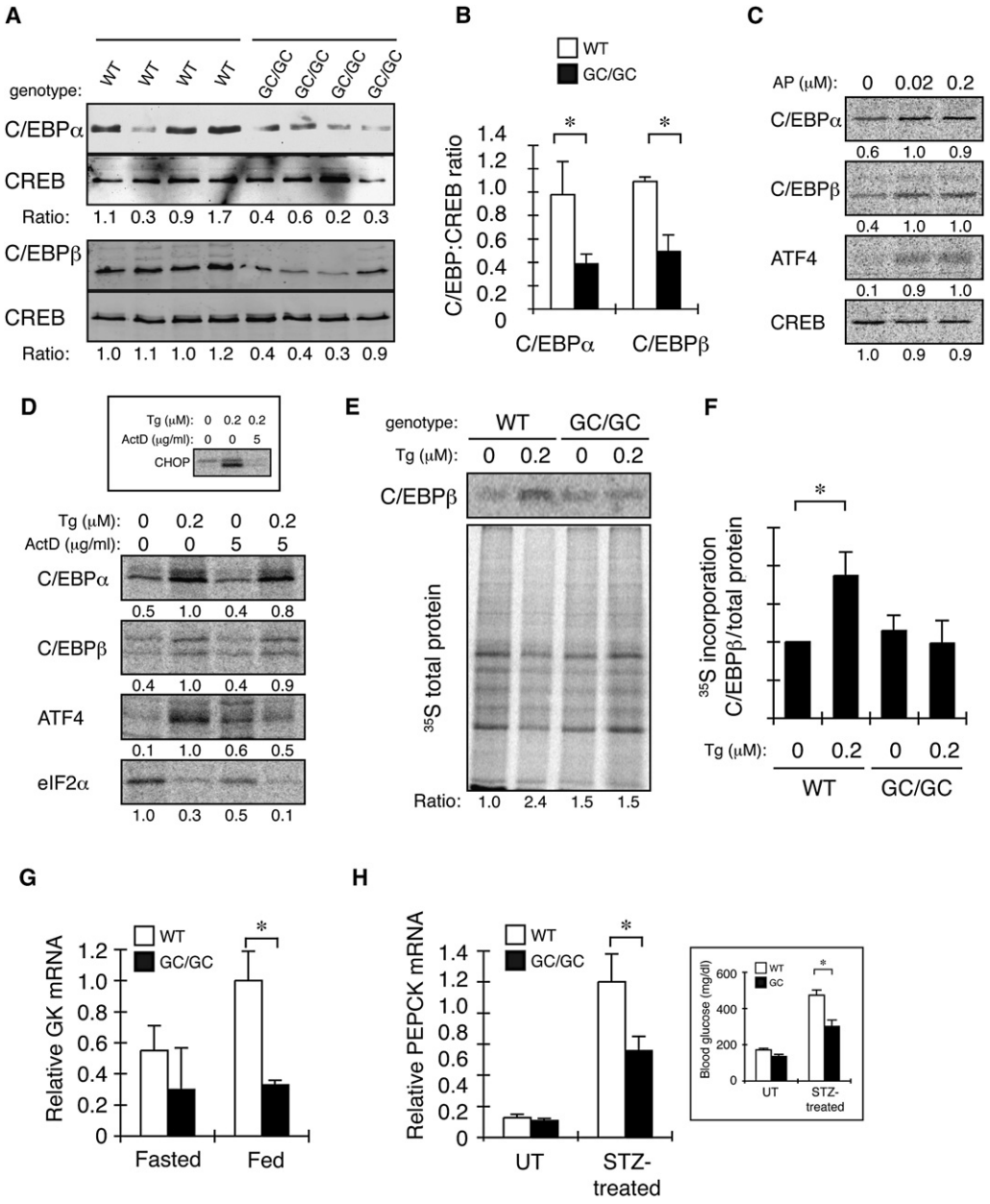

Figure 5. Translational Upregulation of C/EBPα and β by the ISR

(A) Immunoblot of C/EBPα, C/EBPβ, and CREB (as a loading control) in nuclear extract of livers of individual animals of the indicated genotypes. The ratio of C/EBP to CREB signal in each sample is indicated.

(B) Graphic presentation of the data in (A) (mean ± SEM, n = 4, *p < 0.05).

(C) Autoradiograph of [^{35}S]methionine/cysteine-labeled endogenous proteins immunoprecipitated from *Fv2E-PERK* transgenic CHO cells after a 30 min labeling pulse in the presence of the indicated concentrations of AP20187 (AP). The relative signal level in each sample is indicated below the panel.

(D) Autoradiograph of [^{35}S]methionine/cysteine-labeled endogenous proteins immunoprecipitated from HepG2 cells after a 30 min labeling pulse in the presence of the indicated concentrations of thapsigargin (Tg) and/or actinomycin D (ActD). The inset is an autoradiogram of CHOP immunoprecipitated from cells exposed to Tg for 6 hr and actinomycin D for 2 hr before the labeling pulse.

(E) Autoradiogram of an experiment identical in design to that in (D), performed on primary hepatocytes obtained from wild-type and *Alb::GC* mice. The upper panel shows metabolically labeled immunopurified C/EBPβ; the lower panel shows metabolically labeled proteins in the cell lysate. The ratio of label incorporated into C/EBPβ versus total protein, normalized to the untreated WT sample, is reported below. Shown is a typical experiment reproduced three times.

(F) Plot of the ratio of labeled C/EBPβ to total protein in all experiments performed on untreated and Tg-treated primary hepatocytes from wild-type and *Alb::GC* transgenic mice (mean ± SEM in arbitrary units, n = 3, *p < 0.05).

(G) Relative levels of glucokinase (GK) mRNA in liver of fasted and fed nontransgenic (WT) and *Alb::GC* transgenic mice (mean ± SEM, n = 3, *p < 0.05).

(H) Relative levels of PEPCK mRNA in liver of untreated (UT) and streptozotocin (STZ)-injected animals of the indicated genotypes (mean ± SEM, n = 3, *p < 0.05). The inset at right shows morning nonfasted blood glucose of the same animals.

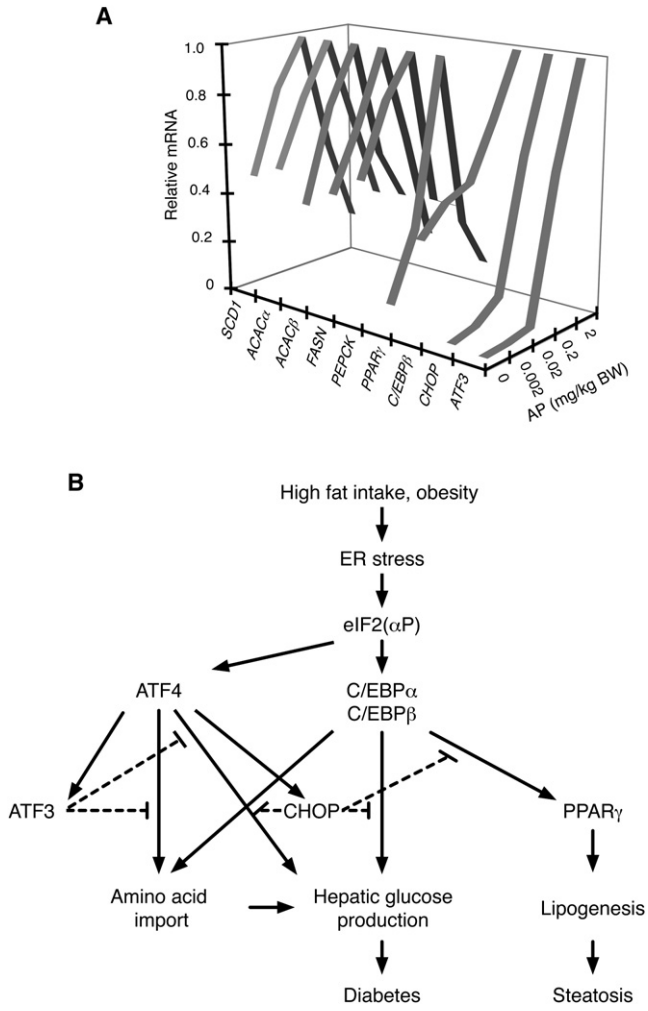

Figure 6. Biphasic Regulation of Genes Involved in Intermediary Metabolism by the ISR

(A) Relative levels of the indicated mRNAs in liver of *Ttr::Fv2E-PERK* transgenic mice 8 hr after i.p. injection of the indicated doses of AP20187 (AP). The complete data set and statistical analysis for this experiment is presented in Table S5.

(B) Summary of interactions between components of the ISR regulating intermediary metabolism.

To determine liver glycogen content, livers (100–150 mg) were digested in 0.3 ml of 30% KOH for 30 min at 100°C, followed by addition of 0.1 ml of 20% $NaSO_4$ and 0.8 ml of ethanol. Macromolecules containing glycogen were precipitated by centrifugation (20,000 × g, 10 min) and washed with 70% ethanol. The pellets were hydrolyzed in 0.5 ml of 4 N H_2SO_4 for 10 min at 100°C and neutralized by 0.5 ml of 4 N NaOH. To measure glucose concentration, 5 μl of the sample supernatant was added in a glucose (HK) assay reagent (Sigma). Liver glycogen concentration was determined by comparison with a standard curve constructed by glycogen from oyster type II (Sigma).

Triglyceride content of liver tissue was measured enzymatically (L-Type TG H test, Wako Pure Chemical Industries) on lipids extracted from tissue samples with chloroform:methanol (2:1 mix).

Histological Analysis

Livers from animals perfused with 10% paraformaldehyde were fixed in the same, paraffin embedded, sectioned in 5 μm slices, and stained with hematoxylin and eosin or periodic acid-Schiff (PAS). Oil red O was used to stain neutral lipids in frozen liver sections. Hepatic steatosis was assessed in three categories—grade, location, and microvesicularity—and a composite score was obtained (based on Kleiner et al., 2005).

RNA Analysis

Livers were snap frozen in liquid nitrogen, and total RNA was isolated using RNA-STAT60 (Tel-Test) and an RNeasy Mini Kit (QIAGEN). For gene expression profiling, total RNA was fluorescently labeled and hybridized to Affymetrix mouse genome 430A 2.0 GeneChip or Affymetrix murine genome U74Av2 GeneChip under standard conditions. Primary image analysis of the arrays was performed using GeneChip 3.2 software (Affymetrix). The raw data from the hybridization experiments were analyzed by GeneSpring GX (Agilent Technologies). The raw signal from each gene was normalized to the mean strength of all genes from the same chip to obtain the normalized signal strength. Then, to allow visualization of all data on the same scale for subsequent analysis, the normalized signal strength of each gene was divided by the median signal strength for that gene among all samples to obtain the normalized expression level.

Quantitative RT-PCR was performed with the iScript One-Step RT-PCR kit using the MyiQ single-color real-time PCR detection system (Bio-Rad Laboratories). All PCR reactions were performed in duplicate or triplicate, and PCR products were subjected to a melting curve analysis. The abundance of specific mRNAs was determined by comparison with a standard curve constructed by serial dilution of the sample and normalized to β-actin. Primers used for PCR reactions are listed in Table S4.

Cell Culture

HepG2 cells were cultured in regular DMEM supplemented with 10% FetalClone II serum (Hyclone) and penicillin-streptomycin. CHO-KI cells were grown in Ham's F12 supplemented with 10% FetalClone II serum and penicillin-streptomycin.

Primary hepatocytes were isolated from wild-type and *Alb::GC* mice, cultured on type I collagen-coated plates in Waymouth's medium supplemented with 0.1 nM insulin, and metabolically labeled as described previously (Oyadomari et al., 2006).

Protein Analysis

PERK and GADD34 were detected in liver lysates by immunoprecipitation followed by immunoblotting as described or by direct immunoblotting of the lysates to detect phosphorylated and total eIF2α as described previously (Harding et al., 2001). C/EBPα, C/EBPβ, and CREB were blotted in a nuclear extract prepared from liver. Antibodies for immunoprecipitation for GADD34 and PERK and immunoblotting procedures for eIF2α, GADD34, PERK, C/EBPα, C/EBPβ, and CREB have been described previously (Batchvarova et al., 1995; Harding et al., 2001; Novoa et al., 2001). Phosphorylated eIF2α was detected using BioSource Ab #44-728G lot #0201.

The translation of C/EBPα, C/EBPβ, ATF4, CREB, and eIF2α was measured by pulse labeling and immunoprecipitation in Fv2E-PERK-expressing CHO cells (Lu et al., 2004a), HepG2 cells, and primary hepatocytes. For metabolic labeling, cells were switched to methionine and cysteine minus DMEM with 10% dialyzed fetal calf serum 5 min before addition of TRAN^{35}S-LABEL (MP Biomedicals) at 400 μCi/ml for 30 min.

Statistical Analysis

All results are expressed as means ± SEM. Unpaired two-tailed Student's t tests were performed to determine p values for paired samples, and two-way ANOVA with repeat measurements was performed to analyze measurements obtained by time course.

ACCESSION NUMBERS

The complete data set for the data reported herein has been submitted to the NCBI GEO database (http://www.ncbi.nlm.nih.gov/geo/) with the accession numbers GSE11116 and GSE11210.

SUPPLEMENTAL DATA

Supplemental Data include five tables and two figures and can be found with this article online at http://www.cellmetabolism.org/cgi/content/full/7/6/520/DC1/.

ACKNOWLEDGMENTS

We thank R. Palmiter (University of Washington) for the pBS-Alb e/p plasmid, D. Accili (Columbia University) for the pTTR-ExV3 plasmid, and ARIAD Inc. for the Fv2E dimerization system and the AP20187 compound. This work was supported by NIH grant DK47119 to D.R. and fellowships from the Uehara Memorial Foundation and the Naito Foundation to S.O.

Received: September 10, 2007
Revised: December 21, 2007
Accepted: April 29, 2008
Published: June 3, 2008

REFERENCES

Allen-Jennings, A.E., Hartman, M.G., Kociba, G.J., and Hai, T. (2002). The roles of ATF3 in liver dysfunction and the regulation of phosphoenolpyruvate carboxykinase gene expression. J. Biol. Chem. *277*, 20020–20025.

Batchvarova, N., Wang, X.-Z., and Ron, D. (1995). Inhibition of adipogenesis by the stress-induced protein CHOP (GADD153). EMBO J. *14*, 4654–4661.

Bernales, S., Papa, F.R., and Walter, P. (2006). Intracellular signaling by the unfolded protein response. Annu. Rev. Cell Dev. Biol. *22*, 487–508.

Calkhoven, C.F., Muller, C., and Leutz, A. (2000). Translational control of C/EBP-Palpha and C/EBPbeta isoform expression. Genes Dev. *14*, 1920–1932.

Chen, C., Dudenhausen, E.E., Pan, Y.X., Zhong, C., and Kilberg, M.S. (2004). Human CCAAT/enhancer-binding protein beta gene expression is activated by endoplasmic reticulum stress through an unfolded protein response element downstream of the protein coding sequence. J. Biol. Chem. *279*, 27948–27956.

Delepine, M., Nicolino, M., Barrett, T., Golamaully, M., Lathrop, G.M., and Julier, C. (2000). EIF2AK3, encoding translation initiation factor 2-alpha kinase 3, is mutated in patients with Wolcott-Rallison syndrome. Nat. Genet. *25*, 406–409.

Deng, J., Lu, P.D., Zhang, Y., Scheuner, D., Kaufman, R.J., Sonenberg, N., Harding, H.P., and Ron, D. (2004). Translational repression mediates activation of nuclear factor kappa B by phosphorylated translation initiation factor 2. Mol. Cell. Biol. *24*, 10161–10168.

Dhahbi, J.M., Mote, P.L., Tillman, J.B., Walford, R.L., and Spindler, S.R. (1997). Dietary energy tissue-specifically regulates endoplasmic reticulum chaperone gene expression in the liver of mice. J. Nutr. *127*, 1758–1764.

Farmer, S.R. (2006). Transcriptional control of adipocyte formation. Cell Metab. *4*, 263–273.

Gavrilova, O., Haluzik, M., Matsusue, K., Cutson, J.J., Johnson, L., Dietz, K.R., Nicol, C.J., Vinson, C., Gonzalez, F.J., and Reitman, M.L. (2003). Liver peroxisome proliferator-activated receptor gamma contributes to hepatic steatosis, triglyceride clearance, and regulation of body fat mass. J. Biol. Chem. *278*, 34268–34276.

Guo, F., and Cavener, D.R. (2007). The GCN2 eIF2alpha kinase regulates fatty-acid homeostasis in the liver during deprivation of an essential amino acid. Cell Metab. *5*, 103–114.

Hao, S., Sharp, J.W., Ross-Inta, C.M., McDaniel, B.J., Anthony, T.G., Wek, R.C., Cavener, D.R., McGrath, B.C., Rudell, J.B., Koehnle, T.J., and Gietzen, D.W. (2005). Uncharged tRNA and sensing of amino acid deficiency in mammalian piriform cortex. Science *307*, 1776–1778.

Harding, H.P., Novoa, I., Zhang, Y., Zeng, H., Wek, R., Schapira, M., and Ron, D. (2000). Regulated translation initiation controls stress-induced gene expression in mammalian cells. Mol. Cell *6*, 1099–1108.

Harding, H.P., Zeng, H., Zhang, Y., Jungreis, R., Chung, P., Plesken, H., Sabatini, D.D., and Ron, D. (2001). Diabetes mellitus and exocrine pancreatic dysfunction in Perk−/− mice reveals a role for translational control in secretory cell survival. Mol. Cell *7*, 1153–1163.

Harding, H.P., Zhang, Y., Zeng, H., Novoa, I., Lu, P.D., Calfon, M., Sadri, N., Yun, C., Popko, B., Paules, R., et al. (2003). An integrated stress response regulates amino acid metabolism and resistance to oxidative stress. Mol. Cell *11*, 619–633.

Hinnebusch, A.G., and Natarajan, K. (2002). Gcn4p, a master regulator of gene expression, is controlled at multiple levels by diverse signals of starvation and stress. Eukaryot. Cell *1*, 22–32.

Hu, C.C., Qing, K., and Chen, Y. (2004). Diet-induced changes in stearoyl-CoA desaturase 1 expression in obesity-prone and -resistant mice. Obes. Res. *12*, 1264–1270.

Jiang, H.Y., Wek, S.A., McGrath, B.C., Scheuner, D., Kaufman, R.J., Cavener, D.R., and Wek, R.C. (2003). Phosphorylation of the alpha subunit of eukaryotic initiation factor 2 is required for activation of NF-kappaB in response to diverse cellular stresses. Mol. Cell. Biol. *23*, 5651–5663.

Jiang, H.Y., Wek, S.A., McGrath, B.C., Lu, D., Hai, T., Harding, H.P., Wang, X., Ron, D., Cavener, D.R., and Wek, R.C. (2004). Activating transcription factor 3 is integral to the eukaryotic initiation factor 2 kinase stress response. Mol. Cell. Biol. *24*, 1365–1377.

Kleiner, D.E., Brunt, E.M., Van Natta, M., Behling, C., Contos, M.J., Cummings, O.W., Ferrell, L.D., Liu, Y.C., Torbenson, M.S., Unalp-Arida, A., et al. (2005). Design and validation of a histological scoring system for nonalcoholic fatty liver disease. Hepatology *41*, 1313–1321.

Lee, A.H., Chu, G.C., Iwakoshi, N.N., and Glimcher, L.H. (2005). XBP-1 is required for biogenesis of cellular secretory machinery of exocrine glands. EMBO J. *24*, 4368–4380.

Liu, S., Croniger, C., Arizmendi, C., Harada-Shiba, M., Ren, J., Poli, V., Hanson, R.W., and Friedman, J.E. (1999). Hypoglycemia and impaired hepatic glucose production in mice with a deletion of the C/EBPbeta gene. J. Clin. Invest. *103*, 207–213.

Lu, P.D., Harding, H.P., and Ron, D. (2004a). Translation re-initiation at alternative open reading frames regulates gene expression in an integrated stress response. J. Cell Biol. *167*, 27–33.

Lu, P.D., Jousse, C., Marciniak, S.J., Zhang, Y., Novoa, I., Scheuner, D., Kaufman, R.J., Ron, D., and Harding, H.P. (2004b). Cytoprotection by pre-emptive conditional phosphorylation of translation initiation factor 2. EMBO J. *23*, 169–179.

Maurin, A.C., Jousse, C., Averous, J., Parry, L., Bruhat, A., Cherasse, Y., Zeng, H., Zhang, Y., Harding, H., Ron, D., and Fafournoux, P. (2005). The GCN2 kinase biases feeding behavior to maintain amino-acid homeostasis in omnivores. Cell Metab. *1*, 273–277.

Millward, C.A., Heaney, J.D., Sinasac, D.S., Chu, E.C., Bederman, I.R., Gilge, D.A., Previs, S.F., and Croniger, C.M. (2007). Mice with a deletion in the gene for CCAAT/enhancer-binding protein beta are protected against diet-induced obesity. Diabetes *56*, 161–167.

Nakatani, Y., Kaneto, H., Kawamori, D., Yoshiuchi, K., Hatazaki, M., Matsuoka, T.A., Ozawa, K., Ogawa, S., Hori, M., Yamasaki, Y., and Matsuhisa, M. (2005). Involvement of endoplasmic reticulum stress in insulin resistance and diabetes. J. Biol. Chem. *280*, 847–851.

Novoa, I., Zeng, H., Harding, H., and Ron, D. (2001). Feedback inhibition of the unfolded protein response by GADD34-mediated dephosphorylation of eIF2α. J. Cell Biol. *153*, 1011–1022.

Novoa, I., Zhang, Y., Zeng, H., Jungreis, R., Harding, H.P., and Ron, D. (2003). Stress-induced gene expression requires programmed recovery from translational repression. EMBO J. *22*, 1180–1187.

Oyadomari, S., Yun, C., Fisher, E.A., Kreglinger, N., Kreibich, G., Oyadomari, M., Harding, H.P., Goodman, A.G., Harant, H., Garrison, J.L., et al. (2006). Cotranslocational degradation protects the stressed endoplasmic reticulum from protein overload. Cell *126*, 727–739.

Ozawa, K., Miyazaki, M., Matsuhisa, M., Takano, K., Nakatani, Y., Hatazaki, M., Tamatani, T., Yamagata, K., Miyagawa, J., Kitao, Y., et al. (2005). The endoplasmic reticulum chaperone improves insulin resistance in type 2 diabetes. Diabetes *54*, 657–663.

Ozcan, U., Cao, Q., Yilmaz, E., Lee, A.H., Iwakoshi, N.N., Ozdelen, E., Tuncman, G., Gorgun, C., Glimcher, L.H., and Hotamisligil, G.S. (2004). Endoplasmic reticulum stress links obesity, insulin action, and type 2 diabetes. Science *306*, 457–461.

Ozcan, U., Yilmaz, E., Ozcan, L., Furuhashi, M., Vaillancourt, E., Smith, R.O., Gorgun, C.Z., and Hotamisligil, G.S. (2006). Chemical chaperones reduce ER stress and restore glucose homeostasis in a mouse model of type 2 diabetes. Science *313*, 1137–1140.

Patil, C.K., Li, H., and Walter, P. (2004). Gcn4p and novel upstream activating sequences regulate targets of the unfolded protein response. PLoS Biol. *2*, E246.

Rahman, S.M., Schroeder-Gloeckler, J.M., Janssen, R.C., Jiang, H., Qadri, I., Maclean, K.N., and Friedman, J.E. (2007). CCAAT/enhancing binding protein beta deletion in mice attenuates inflammation, endoplasmic reticulum stress, and lipid accumulation in diet-induced nonalcoholic steatohepatitis. Hepatology *45*, 1108–1117.

Ron, D., and Habener, J.F. (1992). CHOP, a novel developmentally regulated nuclear protein that dimerizes with transcription factors C/EBP and LAP and functions as a dominant negative inhibitor of gene transcription. Genes Dev. *6*, 439–453.

Ron, D., and Harding, H. (2007). eIF2a phosphorylation in cellular stress responses and disease. In Translational Control, N. Sonenberg, J. Hershey, and M. Mathews, eds. (Cold Spring Harbor, NY, USA: Cold Spring Harbor Laboratory Press), pp. 345–368.

Rosen, E.D., Walkey, C.J., Puigserver, P., and Spiegelman, B.M. (2000). Transcriptional regulation of adipogenesis. Genes Dev. *14*, 1293–1307.

Rutkowski, D.T., Arnold, S.M., Miller, C.N., Wu, J., Li, J., Gunnison, K.M., Mori, K., Sadighi Akha, A.A., Raden, D., and Kaufman, R.J. (2006). Adaptation to ER stress is mediated by differential stabilities of pro-survival and pro-apoptotic mRNAs and proteins. PLoS Biol. *4*, e374.

Schadinger, S.E., Bucher, N.L., Schreiber, B.M., and Farmer, S.R. (2005). PPARgamma2 regulates lipogenesis and lipid accumulation in steatotic hepatocytes. Am. J. Physiol. Endocrinol. Metab. *288*, E1195–E1205.

Scheuner, D., Song, B., McEwen, E., Gillespie, P., Saunders, T., Bonner-Weir, S., and Kaufman, R.J. (2001). Translational control is required for the unfolded protein response and in vivo glucose homeostasis. Mol. Cell *7*, 1165–1176.

Scheuner, D., Mierde, D.V., Song, B., Flamez, D., Creemers, J.W., Tsukamoto, K., Ribick, M., Schuit, F.C., and Kaufman, R.J. (2005). Control of mRNA translation preserves endoplasmic reticulum function in beta cells and maintains glucose homeostasis. Nat. Med. *11*, 757–764.

Schroder, M., and Kaufman, R.J. (2005). The mammalian unfolded protein response. Annu. Rev. Biochem. *74*, 739–789.

Schroder, M., Chang, J.S., and Kaufman, R.J. (2000). The unfolded protein response represses nitrogen-starvation induced developmental differentiation in yeast. Genes Dev. *14*, 2962–2975.

Schroeder-Gloeckler, J.M., Rahman, S.M., Janssen, R.C., Qiao, L., Shao, J., Roper, M., Fischer, S.J., Lowe, E., Orlicky, D.J., McManaman, J.L., et al. (2007). CCAAT/enhancer-binding protein beta deletion reduces adiposity, hepatic steatosis, and diabetes in Lepr(db/db) mice. J. Biol. Chem. *282*, 15717–15729.

Shen, X., Ellis, R.E., Lee, K., Liu, C.-Y., Yang, K., Solomon, A., Yoshida, H., Morimoto, R., Kurnit, D.M., Mori, K., and Kaufman, R.J. (2001). Complementary signaling pathways regulate the unfolded protein response and are required for *C. elegans* development. Cell *107*, 893–903.

Vattem, K.M., and Wek, R.C. (2004). Reinitiation involving upstream ORFs regulates ATF4 mRNA translation in mammalian cells. Proc. Natl. Acad. Sci. USA *101*, 11269–11274.

Wang, N.D., Finegold, M., Bradley, A., Ou, C., Abdelsayed, S., Wilde, M., Taylor, L., Wilson, D., and Darlington, G. (1995). Impaired energy homeostasis in C/EBPα knockout mice. Science *269*, 1108–1112.

Wu, J., Rutkowski, D.T., Dubois, M., Swathirajan, J., Saunders, T., Wang, J., Song, B., Yau, G.D., and Kaufman, R.J. (2007). ATF6alpha optimizes long-term endoplasmic reticulum function to protect cells from chronic stress. Dev. Cell *13*, 351–364.

Yamamoto, K., Sato, T., Matsui, T., Sato, M., Okada, T., Yoshida, H., Harada, A., and Mori, K. (2007). Transcriptional induction of mammalian ER quality control proteins is mediated by single or combined action of ATF6alpha and XBP1. Dev. Cell *13*, 365–376.

Zhang, P., McGrath, B., Li, S., Frank, A., Zambito, F., Reinert, J., Gannon, M., Ma, K., McNaughton, K., and Cavener, D.R. (2002). The PERK eukaryotic initiation factor 2 alpha kinase is required for the development of the skeletal system, postnatal growth, and the function and viability of the pancreas. Mol. Cell. Biol. *22*, 3864–3874.